Journal of Materials Chemistry C

COMMUNICATION

View Article Online
View Journal

Cite this: DOI: 10.1039/c4tc02136c

Received 22nd September 2014
Accepted 4th November 2014

DOI: 10.1039/c4tc02136c

www.rsc.org/MaterialsC

Ferroelectricity in Dion–Jacobson $ABiNb_2O_7$ (A = Rb, Cs) compounds†

Chen Chen,[a] Huanpo Ning,[a] Serban Lepadatu,[b] Markys Cain,[b] Haixue Yan[a] and Mike J. Reece*[a]

The ferroelectric properties of 2-layer Dion–Jacobson compounds $ABiNb_2O_7$ (A = Rb and Cs) were studied. Ferroelectricity and piezoelectricity of $CsBiNb_2O_7$ were demonstrated for the first time. The ferroelectric domain structure of Dion–Jacobson compounds were imaged using PFM. The Curie points of $RbBiNb_2O_7$ and $CsBiNb_2O_7$ are 1098 ± 5 and 1033 ± 5 °C, respectively. The piezoelectric constant of $RbBiNb_2O_7$ and $CsBiNb_2O_7$ are approximately 5 and 8 pC N^{-1}. Thermal depoling was also studied to confirm the Curie temperature and the stability of the piezoelectricity.

Perovskite-like layered structured (PLS) compounds display a range of interesting physical and chemical properties, including photocatalysis, photoluminescence, ion conductivity, electrochemical stability, magnetic properties, ferroelectricity and piezoelectricity.[1–7] Generally, the perovskite layers of PLS materials are formed by corner-sharing BO_6 octahedra separated by oxygen rich layers. There are mainly three homologous series of PLS materials according to their different BO_6 octahedra orientation: the Dion–Jacobson type phases ($A'A_{n-1}BnO_{3n+1}$); the $A_nB_nO_{3n+2}$ type phases; and the hexagonal phases ($A_nB_{n-1}O_{3n}$).[1] The crystal structure of Dion–Jacobson phase can be regarded as a result of cutting the idealized perovskite structure across the $(1\ 0\ 0)_{perovskite}$ plane, and the crystal structure of $A_nB_nO_{3n+2}$ phase and the hexagonal phase can be regarded as a result of cutting the perovskite structure across the $(1\ 1\ 0)_{perovskite}$ and $(1\ 1\ 1)_{perovskite}$ planes, respectively.[1,8] The $A_nB_nO_{3n+2}$ type PLS materials have been shown to be ferroelectrics with super high Curie point, especially the 4-layer $La_2Ti_2O_7$ and $Sr_2Nb_2O_7$ phases, which have Curie point above 1300 °C.[9–11] However, materials with Dion–Jacobson structure and Hexagonal structure have rarely been reported to present ferroelectricity.

The crystal structure of the Dion–Jacobson compound $CsBiNb_2O_7$ was studied by Snedden, *et al.* and found to have similar structural distortions to that of ferroelectric Aurivillius phase $SrBi_2Ta_2O_9$, but they concluded that $CsBiNb_2O_7$ does not display ferroelectricity according to dielectric measurements.[12,13] Recently, Fennie *et al.* demonstrated the polar nature of $CsBiNb_2O_7$ using first principles and group theoretical analysis and estimated that $CsBiNb_2O_7$ has a spontaneous polarization of 40 μC cm^{-2}.[14] More recently, Goff *et al.* reported that the ferroelectricity of $CsBiNb_2O_7$ cannot be detected due to its large leakage current and significant proton conductivity.[15] Recently, the ferroelectricity and piezoelectricity of $RbBiNb_2O_7$, which has similar crystal structure to $CsBiNb_2O_7$, was reported by Li *et al.*,[16] which made us to reconsider the possibility of discovering ferroelectricity for $CsBiNb_2O_7$.

In this work, we present the ferroelectricity and piezoelectricity of $ABiNb_2O_7$ (A = Rb, Cs) ceramics by direct evidence of ferroelectric domain switching and piezoelectric activity. The ferroelectric domain structures of $CsBiNb_2O_7$ and $RbBiNb_2O_7$ were investigated using PFM images. The Curie point for $CsBiNb_2O_7$ and $RbBiNb_2O_7$ were found to be 1033 ± 5 and 1098 ± 5 °C by studying the temperature dependence of permittivity and thermal depoling.

Fig. 1 shows the XRD patterns of $ABiNb_2O_7$ powders measured at room temperature. Both the powders of $CsBiNb_2O_7$ and $RbBiNb_2O_7$ are single phase, and no impurity can be observed in the XRD patterns. $CsBiNb_2O_7$ and $RbBiNb_2O_7$ have the same 2-layer Dion–Jacobson structure at room temperature, which is orthorhombic and belongs to space group $P2_1am$ (26).[13,14,16] The lattice parameters are a = 5.4964, b = 5.4223 and c = 11.3704 Å for $CsBiNb_2O_7$ and a = 5.4193, b = 5.3589 and c = 11.2099 Å for $RbBiNb_2O_7$. Their spontaneous polarization directions are along the a-axis. The insets in Fig. 1 show the SEM images of the plate-like powders. Due to the plate-like grain shape, preferred orientation of the $(0\ 0\ l)$ plane can be observed in the powders. After SPS sintering, greater preferred

[a]School of Engineering and Materials Science, Queen Mary University of London, London E1 4NS, UK. E-mail: m.j.reece@qmul.ac.uk

[b]National Physical Laboratory, Teddington, Middlesex TW11 0LW, UK

† Electronic supplementary information (ESI) available: Experimental procedure, XRD results of sintered ceramics, PFM of $RbBiNb_2O_7$. See DOI: 10.1039/c4tc02136c

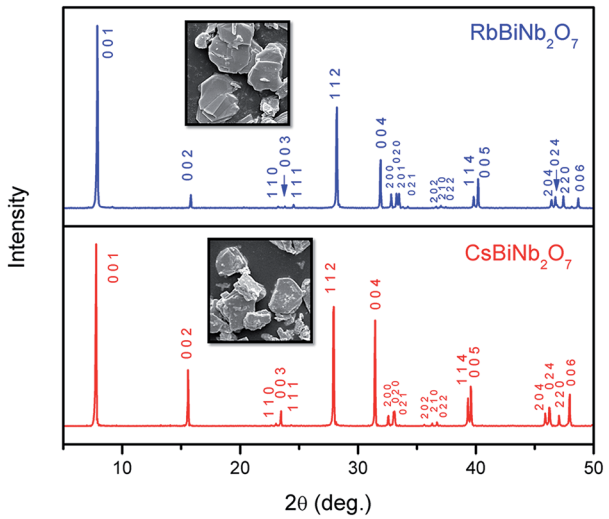

Fig. 1 X-ray diffraction patterns of $ABiNb_2O_7$ powders.

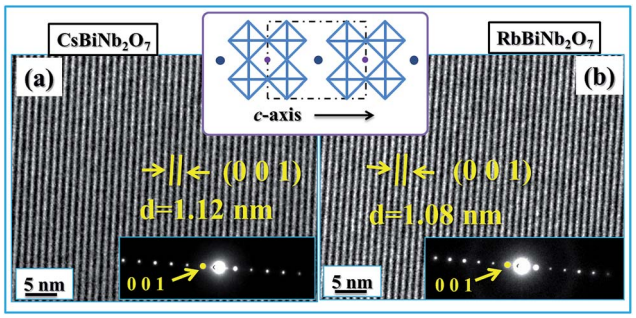

Fig. 2 HRTEM images of $ABiNb_2O_7$ ceramics: (a) $CsBiNb_2O_7$; (b) $RbBiNb_2O_7$.

(0 0 *l*) orientation was found in the ceramics (Fig. S1†). The orientation factors for $CsBiNb_2O_7$ and $RbBiNb_2O_7$ ceramic were 0.9 and 0.7, respectively. The benefit of orientation is to decrease the coercive field for polarization switching.

Fig. 2 shows the HRTEM images of $ABiNb_2O_7$ ceramics. Unfaulted lattice planes were observed for both $CsBiNb_2O_7$ (Fig. 2(a)) and $RbBiNb_2O_7$ (Fig. 2(b)). The *d*-pacing of the lattice planes was measured to be 1.12 ± 0.02 nm for $CsBiNb_2O_7$ and 1.08 ± 0.02 nm for $RbBiNb_2O_7$. Selected area electron diffraction patterns are shown in insets in Fig. 2(a) and (b). The linear reflections were indexed to be (0 0 *l*) lattice planes. The *d*-spacing of the (0 0 *l*) plane, which corresponds to the length of *c* axis of the unit cell, was measured to be 1.13 ± 0.02 nm for $CsBiNb_2O_7$ and 1.10 ± 0.02 nm for $RbBiNb_2O_7$.

Fig. 3 shows vertical-mode PFM images of $CsBiNb_2O_7$ ceramic. Because the SPS sintered ceramics were highly textured on the (0 0 *l*) plane and the polar axis is in the *a*-direction, samples with surfaces perpendicular to SPS pressing direction were prepared to investigate the ferroelectric domain structure with PFM. Several grains with clear grain boundaries can be observed in the topography image shown in Fig. 3(a). Ferroelectric domain morphology is clearly observed

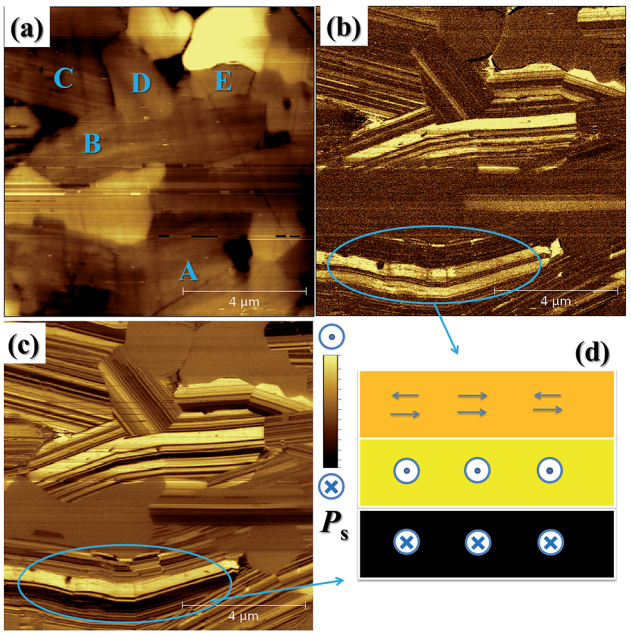

Fig. 3 Vertical-mode PFM images of $CsBiNb_2O_7$ ceramic: (a) topography; (b) amplitude; (c) phase and (d) schematic of the selected area from (c).

in the PFM amplitude and phase images (Fig. 3(b) and (c)). Bright areas in the amplitude image reveal the stripe domains with vertical piezo-response signal. Some of the dark areas reveal regions with in-plane polarization. The bright and dark areas in the phase image reveal the up and down out-of-plane polarization, respectively. Comparing the PFM amplitude and phase images with the topography image, clear ferroelectric domains can be observed in several grains (A to E), and stripe domains with different orientations show strong contrast in each grain. Fig. 3(d) shows the schematic of the out-of-plane and in-plane polarization in grain A. The black, yellow and orange stripes represent the dark, bright and grey areas. The polarization direction can be indexed through comparing the phase and amplitude images. The width of the domains was typically from 10 to 600 nm. Similar ferroelectric domain structure was also observed for $RbBiNb_2O_7$ ceramic (Fig. S2†).

The temperature dependence of dielectric constants of $CsBiNb_2O_7$ and $RbBiNb_2O_7$ are shown in Fig. 4(a). The Curie point, T_c, of $CsBiNb_2O_7$ and $RbBiNb_2O_7$ are 1033 ± 5 and 1098 ± 5 °C, respectively. The ferroelectric-to-paraelectric phase transition temperature for $CsBiNb_2O_7$ is demonstrated for the first time. Goff *et al.* reported that the orthorhombic phase of $CsBiNb_2O_7$ was stable from room temperature to 900 °C and no ferroelectric orthorhombic to paraelectric tetragonal phase transition was observed using high-temperature XRD,[15] which is in agreement with our result that the T_c of $CsBiNb_2O_7$ is above 900 °C (~1033 °C). The T_c of $RbBiNb_2O_7$ was first reported to be 943 °C by Li *et al.*,[16] which is about 155 °C lower than our result. To calibrate our equipment, the T_c of $LiNbO_3$ single crystal was measured with the same equipment. The T_c of $LiNbO_3$ was measured as ~1138 °C. According to the literature,[17] the T_c of

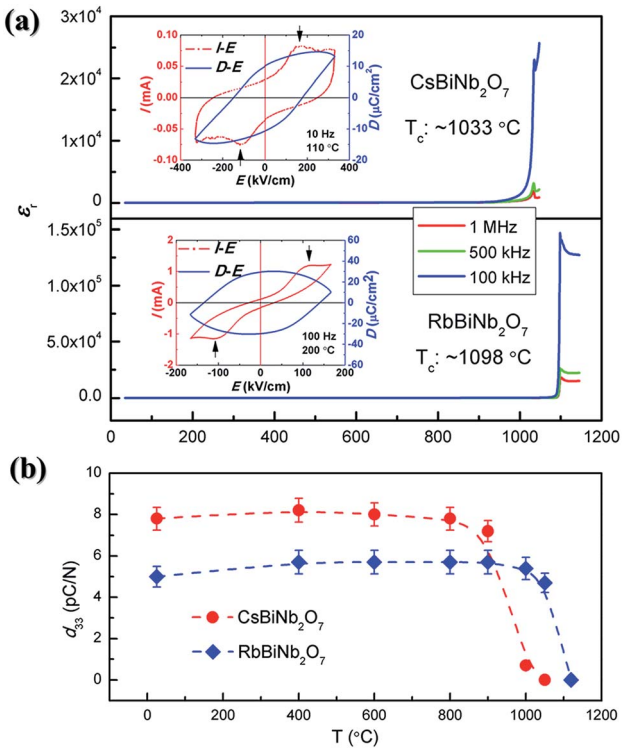

Fig. 4 (a) Temperature dependence of dielectric constant; insets: *I–E* and *D–E* hysteresis loops; (b) thermal depoling results.

single crystal $LiNbO_3$ is 1140 °C, which means that the T_c values we measured are relatively accurate. The insets of Fig. 4(a) show the current–electric field (*I–E*) and electric displacement–electric field (*D–E*) hysteresis loops of $CsBiNb_2O_7$ and $RbBiNb_2O_7$. The *I–E* and *D–E* loops were measured at 110 °C and 10 Hz for $CsBiNb_2O_7$. A typical, unsaturated, ferroelectric *D–E* loop obtained for $CsBiNb_2O_7$ is shown in the inset of Fig. 4(a). In its *I–E* loop, a current peak (marked by arrow) produced by ferroelectric domain switching is observed. For $RbBiNb_2O_7$, *I–E* and *D–E* loops, measured at 200 °C and 100 Hz, are shown in the inset of Fig. 4(a). A typical vesica piscis-shaped *D–E* loop due to leakage current was observed, but the ferroelectric domain switching is demonstrated by the peak observed in the *I–E* loop.

$CsBiNb_2O_7$ and $RbBiNb_2O_7$ have similar polar orthorhombic structure $P2_1am$. Due to the off-centre displacements of A-site Bi ions and octahedral tilting of NbO_6, a spontaneous polarization develops along their *a*-axis. Recently Benedek reported that the origin of ferroelectricity in polar oxides with Dion–Jacobson phases is induced by a combination of octahedral distortions and cation ordering.[18] The macroscopic polarizations of $CsBiNb_2O_7$ and $RbBiNb_2O_7$ were both reported to be 48 μC cm^{-2} using symmetry principles, crystal chemical models, and first-principles calculations. Here the spontaneous polarization was calculated to be 43.8 μC cm^{-2} for $CsBiNb_2O_7$ and 47 μC cm^{-2} for $RbBiNb_2O_7$ according to Shimakawa's model,[19,20] which is in good agreement with Benedek's report. The measured piezoelectric constant d_{33} at room temperature was 8 ± 0.5 pC N^{-1} for $CsBiNb_2O_7$ and 5 ± 0.5 pC N^{-1} for $RbBiNb_2O_7$. Fig. 4(b) shows the thermal depoling results for poled $CsBiNb_2O_7$ and $RbBiNb_2O_7$. All the samples poled at room temperature were annealed at different temperatures for 2 hours. Then their d_{33} values were measured at room temperature. For both $CsBiNb_2O_7$ and $RbBiNb_2O_7$, their d_{33} values are very stable with increasing depoling temperature. The d_{33} starts to drop when the depoling temperature is close to T_c and tends to zero above T_c.

In summary, highly textured 2-layer Dion–Jacobson ceramics $ABiNb_2O_7$ (A = Rb and Cs) were prepared by one-step spark plasma sintering with pressure due to their layered crystal structure, which was demonstrated using XRD. High resolution TEM showed well ordered (0 0 1) lattice planes. Striped ferroelectric domains were observed using PFM. The ferroelectricity and piezoelectricity of $CsBiNb_2O_7$ has been demonstrated for the first time. The T_c of $RbBiNb_2O_7$ and $CsBiNb_2O_7$ are 1098 ± 5 and 1033 ± 5 °C, respectively. The piezoelectric constant of $RbBiNb_2O_7$ and $CsBiNb_2O_7$ were approximately 5 and 8 pC N^{-1}. Thermal depoling studies confirmed the T_c measurements and the stability of the piezoelectricity.

Acknowledgements

The Innovation Research and Development Programme of the Department of Business, Innovation and Skills, UK is acknowledged. Chen thanks China Scholarship Council (CSC) for supporting his PhD studies.

Notes and references

1 F. Lichtenberg, A. Herrnberger and K. Wiedenmann, *Prog. Solid State Chem.*, 2008, **36**, 253.
2 F. Lichtenberg, A. Herrnberger, K. Wiedenmann and J. Mannhart, *Prog. Solid State Chem.*, 2001, **29**, 1.
3 S. Zhang and F. Yu, *J. Am. Ceram. Soc.*, 2011, **94**, 3153.
4 M. Nyman, M. A. Rodriguez, L. E. S. Rohwer, J. E. Martin, M. Waller and F. E. Osterloh, *Chem. Mater.*, 2009, **21**, 4731.
5 T. Wang, C. N. Henderson, T. I. Draskovic and T. E. Mallouk, *Chem. Mater.*, 2013, **26**, 898.
6 D. G. Cahill, A. Melville, D. G. Schlom and M. A. Zurbuchen, *Appl. Phys. Lett.*, 2010, **96**, 121903.
7 T. Ukita, Y. Hirose, S. Ohno, K. Hatabayashi, T. Fukumura and T. Hasegawa, *J. Appl. Phys.*, 2012, **111**, 07D909.
8 I. Levin and L. A. Bendersky, *Acta Crystallogr., Sect. B: Struct. Sci.*, 1999, **55**, 853.
9 S. Nanamatsu, M. Kimura, K. Doi, S. Matsushita and N. Yamada, *Ferroelectrics*, 1974, **8**, 511.
10 H. Yan, H. Ning, Y. Kan, P. Wang and M. J. Reece, *J. Am. Ceram. Soc.*, 2009, **92**, 2270.
11 H. Ning, H. Yan and M. J. Reece, *J. Am. Ceram. Soc.*, 2010, **93**, 1409.
12 M. A. Subramanian, J. Gopalakrishnan and A. W. Sleight, *Mater. Res. Bull.*, 1988, **23**, 837.
13 A. Snedden, K. S. Knight and P. Lightfoot, *J. Solid State Chem.*, 2003, **173**, 309.
14 C. J. Fennie and K. M. Rabe, *Appl. Phys. Lett.*, 2006, **88**, 262902.

15 R. J. Goff, D. Keeble, P. A. Thomas, C. Ritter, F. D. Morrison and P. Lightfoot, *Chem. Mater.*, 2009, **21**, 1296.
16 B.-W. Li, M. Osada, T. C. Ozawa and T. Sasaki, *Chem. Mater.*, 2012, **24**, 3111.
17 P. K. Gallagher, H. M. O'Bryan and C. D. Brandle, *Thermochim. Acta*, 1988, **133**, 1.
18 N. A. Benedek, *Inorg. Chem.*, 2014, **53**, 3769.
19 H. Yan, H. Zhang, R. Ubic, M. J. Reece, J. Liu, Z. Shen and Z. Zhang, *Adv. Mater.*, 2005, **17**, 1261.
20 Y. Shimakawa, Y. Kubo, Y. Nakagawa, S. Goto, T. Kamiyama, H. Asano and F. Izumi, *Phys. Rev. B: Condens. Matter Mater. Phys.*, 2000, **61**, 6559.

